Available online at www.eccomasproceedia.org
Eccomas Proceedia COMPDYN (2019) 3114-3128

ECCOMAS
Proceedia

COMPDYN 2019
7th ECCOMAS Thematic Conference on
Computational Methods in Structural Dynamics and Earthquake Engineering
M. Papadrakakis, M. Fragiadakis (eds.)
Crete, Greece, 24–26 June 2019

NUMERICAL MODELING OF MASONRY-INFILLED RC FRAME STRENGTHENED WITH TRM

Christiana A. Filippou[1], Christis Z. Chrysostomou[2] and Nicholas C. Kyriakides[3]

[1] PhD Candidate, Department of Civil Engineering & Geomatics, Cyprus University of Technology Limassol, Cyprus. Email: filippouch@gmail.com

[2] Professor, Department of Civil Engineering & Geomatics, Cyprus University of Technology, 3603 Limassol, Cyprus. Email: c.chrysostomou@cut.ac.cy

[3] Lecturer, Department of Civil Engineering & Geomatics, Cyprus University of Technology, 3603 Limassol, Cyprus. Email: nicholas.kyriakides@cut.ac.cy

Abstract

The behaviour of masonry-infilled reinforced concrete (RC) frame structures during an earthquake has attracted the attention by structural engineers since the 1950's. During the last decade, the use of textile reinforced mortar (TRM) as strengthening material for masonry-infilled RC frames under in-plane lateral loadings has been studied.

This paper presents a numerical model of the behaviour of existing masonry-infilled RC frame strengthened with TRM that was studied experimentally at the University of Patras. It was a 2:3 scale three-story structure with non-seismic design and detailing, subjected to in-plane cyclic loading through displacement control analysis. The objective of the present study is to identify suitable numerical constitutive models for each component of the structural system, in order to create a numerical tool to model the TRM strengthened-masonry infilled RC frames in-plane behaviour. A 2D TRM strengthened-masonry-infilled RC frame was developed in DIANA finite element analysis (FEA) software and an eigenvalue and nonlinear structural cyclic analysis were performed.

There is good agreement between the numerical model and experimental results. It has been found that the numerical model has the capability to predict the initial stiffness, the ultimate stiffness, the maximum shear-force capacity, cracking patters and the possible failure mode of masonry-infilled RC frame with retrofitting. This model proves to be a reliable model of the behaviour of TRM strengthened- masonry-infilled RC frame under cyclic loading and can be used for further parametric studies.

Keywords: Masonry infills, Textile reinforced mortar, Cyclic loading, Finite element, Numerical modelling, Constitutive model

ISSN:2623-3347
Peer-review under responsibility of the organizing committee of COMPDYN 2019.
doi: 10.7712/120119.7136.19665

1 INTRODUCTION

Masonry-infilled RC frame structures are widely dispersed around the world. Past studies have shown that the in-plane strength and stiffness of the infill walls have influence on the global performance of a structure, subjected to seismic loads. The existence of infill walls in a RC frame can increase the strength, stiffness (relative to a bare frame) [1] and lateral capacity of the building [2]–[4] and at the same time it can introduce brittle shear failure mechanisms associated with the wall failure and wall-frame interaction.

The failure mechanism and the load resistance of a masonry-infilled RC frame depend on the strength and stiffness of an infill with respect to those of the bounding frame. It is known that masonry structures are vulnerable to both in-plane and out-of-plane movements under the action of lateral loads. The in-plane and out-of-plane behavior of the masonry infill has been studied experimentally [5] and numerically [6]. The out-of-plane failures turn out to be more disastrous than the in-plane ones[7]. The in-plane failure mechanisms of masonry-infilled RC frames are identified according to ATC 43 [8], Asteris et al. [9] and Shing and Mehrabi [10]. The infill wall fails in a variety of modes, most often involving some combination of bed joint sliding, corner crushing, diagonal cracking (due to diagonal orientation of the tensile-compressive principal stress), diagonal compression [11] and frame failure modes. The exact mode of failure depends upon material properties, such as compressive strength, shear strength and friction and upon geometric constraints, such as frame-wall interface or window openings and other characteristics. In addition, infill walls in RC structures may cause several undesirable failure mechanisms under seismic loading due to the large concentration of ductility demand in a few members of the structure. For instance, the soft-story mechanism (concentration of inter-story drift demand and damage is in the first story) [12]), the short-column mechanisms (ductility demands on RC columns) [13]), and plan-torsion mechanisms (when infills are unsymmetrically located in plan). The negative effects are associated with plan or vertical irregularities introduced by the infill panels [14,15]. Fig. **1(a)** and **1(b)** illustrate the soft-story and short-column failure mechanism respectively.

(a) (b)

Figure 1: a) Soft-story mechanism [14] and b) Short-column mechanisms [15].

Seismic rehabilitation of existing structural or non-structural elements is a challenging engineering problem nowadays. Several retrofitting techniques have been proposed in order to increase the strength, stiffness, deformation capacity and the ductility of masonry-infilled RC frame structures [16,17]. Most retrofitting techniques include an external coating or overlay to

one or both sides of the infill wall. The most recent retrofitting techniques include the use of fiber reinforced polymers (FRP) [18,19,20,21,22,23,24,25,26] ductile-fiber-reinforced cementitious composites (FRCM) [27,28,29] and textile reinforced mortar (TRM) [30,31]. TRM jacketing is an extremely promising solution for the strengthening of unreinforced infill walls subjected to either out-of-plane or in-plane loading [5]. In recent experimental and numerical studies provided by Koutas et al. [32,33] the use of TRM for strengthening masonry-infilled frames was studied. The study showed that in the retrofitted specimen an approximately 56% increase in the lateral strength, accompanied with a 52% higher deformation capacity at the top of the structure at ultimate strength state was achieved compared to the unretrofitted one. In addition, the TRM retrofitted specimen dissipated 22.5% more energy compared to the unretrofitted one, for the same loading history. Moreover, it was concluded that further studies are needed on masonry-infilled RC frame strengthened with TRM, due to the fact that this method is a newly established technique and the research is limited on this topic.

The purpose of this paper is to simulate the behavior of masonry-infilled RC frame strengthened with TRM under cyclic loading. To achieve this, 2D TRM-masonry-infilled RC frame model was developed in DIANA finite element analysis (FEA) software, using meso-level approach for modelling the infill wall, and an eigenvalue and nonlinear structural cyclic analysis were performed. The present study identifies suitable numerical constitutive models of each component of the structural system in order to create a numerical tool to model masonry infilled RC frames strengthened with TRM under in-plane cyclic loading. The calibration was based on the experimental test performed by Koutas [32] in his PhD study at the University of Patras.

2 DESCRIPTION OF EXPERIMENTAL CASE STUDY

In the experimental case-study carried out by Koutas et al. [32] the effectiveness of seismic retrofitting of existing masonry-infilled RC frames with TRM was studied. It was a 2:3 scale three-storey masonry-infilled RC frame with non-seismic design and detailing subjected to in-plane cyclic loading. Two masonry-infilled frames were designed and built with and without TRM (control specimen). In this part of the paper some details of the experimental case study regarding the masonry-infilled RC frame with the strengthening material TRM are presented for the benefit of the reader. Full details about the experimental case study can be found in Koutas et al. [32] [33].

2.1 Geometry of TRM strengthened masonry-infilled RC frame

The geometry of the masonry-infilled frame is shown in Fig.(**2a**). The columns were of rectangular cross section 170 × 230 mm and the beams were T-section. The column longitudinal reinforcement consisted of Y12 deformed bars lap-spliced only at the base of the first story. The transverse reinforcement for all concrete members consisted of Y6 plain bars with 90° hooks at the ends. The thickness of the concrete cover to stirrups was 10 mm. The infill had a length-to-height aspect ratio 1.36. The infill wall was constructed from perforated, fired clay bricks. The perforations of the bricks were running parallel to the unit's length in the x-direction. The infill wall was composed of two independent wythes separated by a 60-mm gap. The wall was supported rigidly by the RC foundation beam plate with dimensions 0.4 x 0.9 x 4.0 m at the bottom of the wall. The strengthening scheme for masonry-infilled RC frame is shown in Fig.(**2b**). The selection of the strengthening scheme was dictated by the behavior of the unretrofitted specimen. The strengthening scheme includes: carbon-TRM fully wrapped at the ends of columns at the first and second stories, glass-TRM externally bonded on the face of

the infill walls as shown in Fig. (**2b**) and in total, 11 and 8 anchors per side were placed at equal spaces along the interfaces (Fig.**2b**).

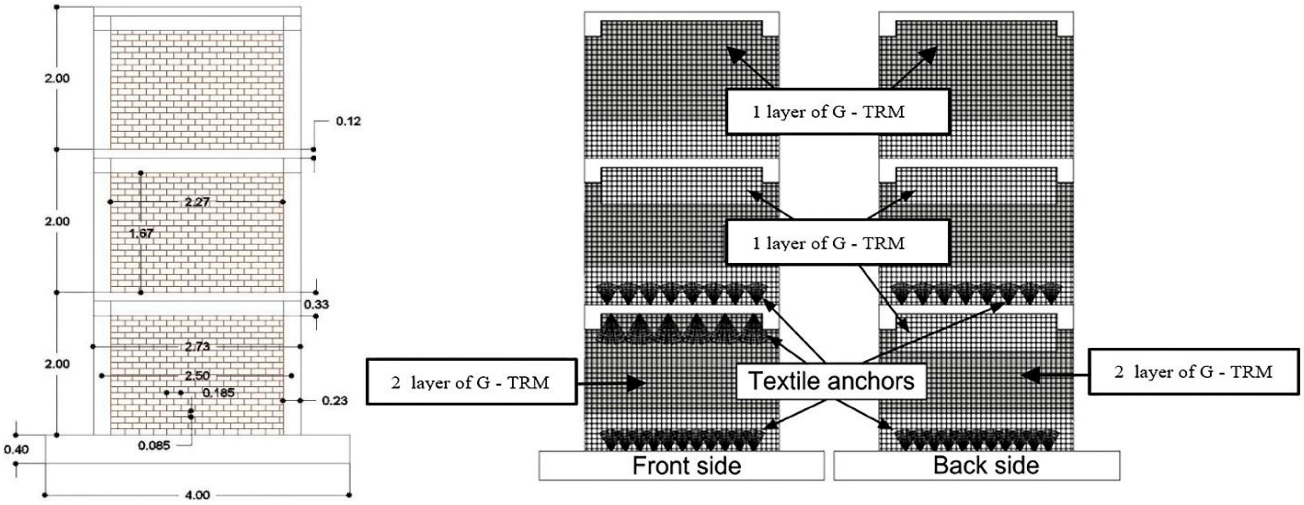

(a) (b)

Figure 2 : (a) Geometry of the masonry-infilled RC frame and (b) Strengthening scheme : textile anchors of first and second story and TRM layer on the faces of masonry infill at the first, second and third story[32].

2.2 Material properties of TRM strengthened masonry-infilled RC frame

For the construction of the RC frame, C25/30 class of concrete was used and the compressive strength of concrete was equal to 27.8 MPa for control specimen and 27.2 MPa for the retrofitted specimen. The modulus of elasticity of the concrete was 24.1 GPa. The longitudinal reinforcement used was class B500C (yield stress equal to 550MPa) deformed steel bars, in the beams and columns, and smooth steel stirrups class S220 (yield stress equal to 270MPa).

Compression and diagonal test on masonry wallets were performed. The compressive strength of the masonry was 5.1 MPa and the elastic modulus of the masonry perpendicular to the bed joints was 3.37GPa. In addition, the mean value of diagonal cracking stress was 0.39 MPa and the shear modulus was 1.38 GPa.

The mortar used as the binding material of the textile was a commercial fiber-reinforced cement-based mortar The mean values of compressive and flexural strength were equal to 18.9 and 4.3 MPa, respectively. The closed carbon-fiber textile TRM jackets were used at the column ends of the first and second story. The tensile strength per running meter and the modulus of elasticity of carbon textile was 157kN/m and 225GPa, respectively. Commercial polymer-coated E-glass textile was used for the infill wall with tensile strength per running meter and modulus of elasticity equal to 115 kN/m and 736GPa, respectively.

2.2 Experimental campaign

The masonry-infilled RC frame with TRM was subjected to a sequence of quasi-static cycles of a predefined force pattern. A history of imposed cycles of displacements was defined to be applied at the top (Fig. **3b**), while maintaining an inverted-triangular distribution of forces to all three floor levels until failure (in terms of global response) occurred. A total of seven cycles were finally applied to TRM strengthened specimen. A general view of the test setup is shown in figure below (Fig. **3a**). Three servo-hydraulic actuators were mounted on the specimen, one per story. The strong foundation beam was fixed to the strong laboratory floor via 16 prestressing rods to provide specimen full clamping. Gravity loading of 80 kN per story

was considered to represent the fraction of permanent loads concurrent to the lateral loading action.

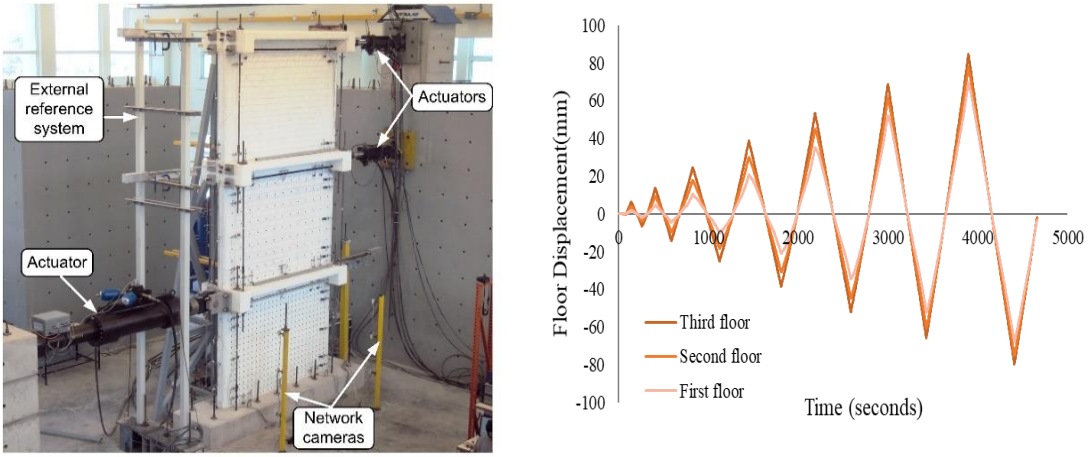

(a) (b)

Figure 3 : (a) Test set up [33] and (b) Imposed cyclic deformation history for all stories [33].

2.3 Experimental results

Free vibration test was performed in RC bare frame and in masonry-infilled RC frame with and without TRM to identify the experimental fundamental period of the structure in each phase of the construction. In order to perform free vibration test, the specimens subjected to a static displacement at the top of the specimen. For all free vibration tests the gravity loading of 80 KN per story was not considered. The fundamental period for masonry-infilled frame with and without TRM was equal to 0.06 and 0.047 seconds, respectively.

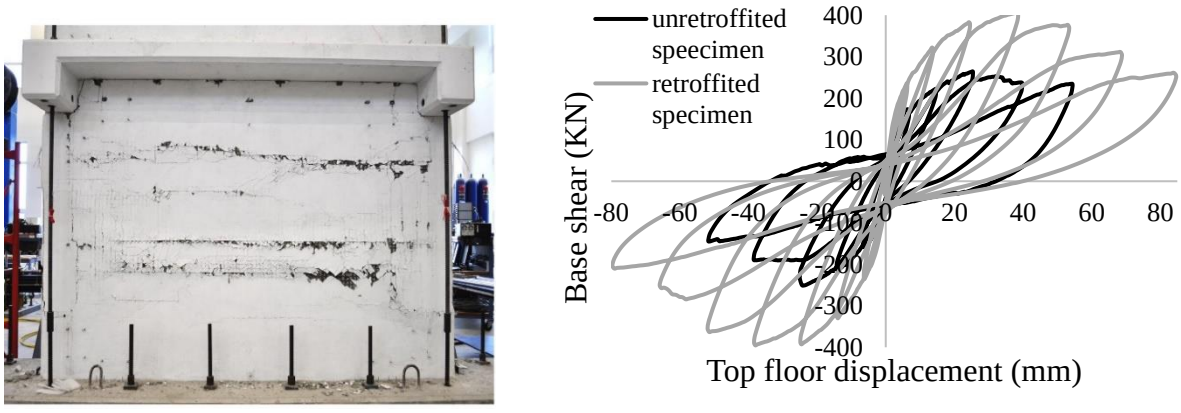

(a) (b)

Figure 4: (a) Failure mode of infilled frame (first floor) at end of the test [32] and (b) Base shear force-displacement hysteresis curve for retrofitted specimen [32].

During early loading in masonry infilled RC frame strengthened with TRM, a dense cracking pattern was developed, with inclined cracks close to the corners of the infill panel and of sliding-type cracks at the central region of the panel at the first floor (Fig.**4a**) and few cracks parallel to the diagonal developed on the second story infill panel. The frame-infill separation occurred at the very early stages of cyclic loading in retrofitted and in unretrofitted specimen and therefore frame-infill separation was not avoided or eliminated after applying the textile layers. The maximum base shear force was attained during the fourth cycle of loading: for the two directions of loading a maximum base shear of 407KN and −395 KN was recorded at

corresponding top displacement of 40 mm and −38 mm (Fig.**4b**). After the fourth cycle of loading, the lateral strength was decreasing due to complete debonding of the TRM from the beam surface on the back side of the first story and local crushing at the first story infill at the two upper ends neighboring the columns.

3 FINITE ELEMENT MODELING OF TRM MASONRY-INFILLED RC FRAME

This study used DIANA FEA software to model the masonry-infilled RC frame strengthened with TRM. The proposed meso-model for TRM strengthened masonry-infilled RC frame was implemented in DIANA FEA using available materials, sections and elements. It is important to be mentioned that the TRM anchors were not modeled. The DIANA FEA was selected for modeling, since it provided the elements, constitutive relationships and materials needed for TRM, concrete and masonry infill [34].

3.1 Constitutive model

In DIANA FEA software there are different available material models to simulate the TRM strengthened masonry-infilled RC frame. In this study, most of the material properties are taken from the experimental case study described above and other material parameters were taken from the literature [35,38]. The numerical results were compared to the experimental results and some parameters were adjusted to achieve reasonable results.

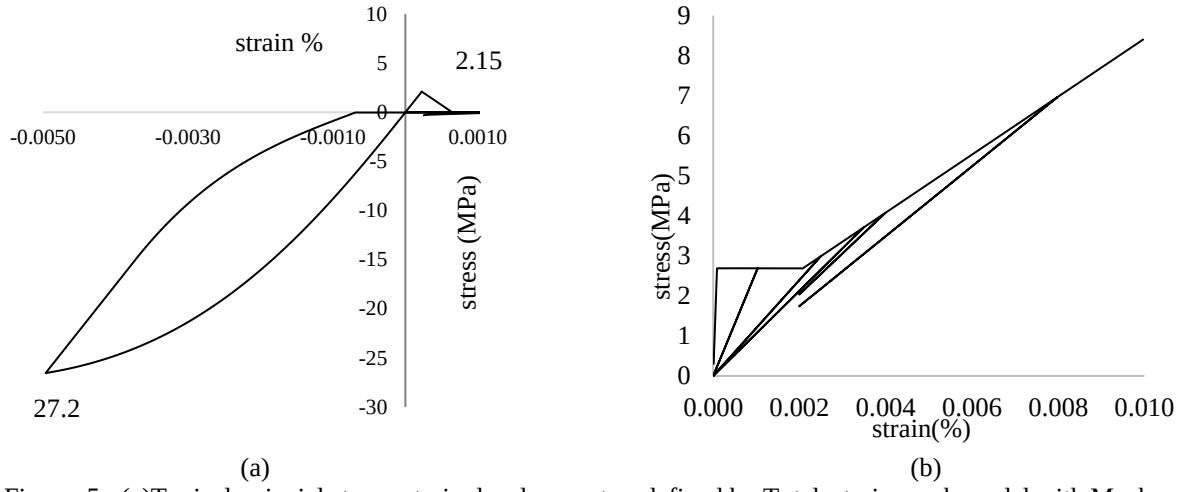

Figure 5 : (a)Typical uniaxial stress–strain development as defined by Total strain crack model with Maekawa Fukuura compressive behavior [43] and (b) Typical uniaxial stress–strain development as defined by Total strain crack model with Fiber reinforced concrete model *(fib)* for tensile behavior and *fib* Concrete Structures 2010 model for the compressive behavior of TRM [35].

The concrete material model that was chosen is the Total Strain Crack model. The Total Strain Crack model [43] describes the tensile and compressive behavior of concrete as shown in Fig. (**5a**). Besides the definition of basic properties like Young's modulus, the Total Strain Crack model requires only a small number of engineering parameters such as the tensile (2.15 MPa) and compressive strength based on the Maekawa Fukuura model [43] (27.2 MPa) and the fracture energy in tension (130 N/m). This model has no ability to reduce the stiffness due to early cracking of the concrete section and therefore the modulus of elasticity was reduced to 9.1 GPa. In addition, the tensile strength and fracture energy were obtained by the empirical equations according to the *fib* model code [35]. In this study, the approach which is used is the

Rotating crack model [36] which is one commonly used approach in which the stress–strain relations are evaluated in the principal directions of the strain vector.

Cyclic performance of RC elements highly depends on the nonlinear response of reinforcing bars under cyclic loading. The Menegotto-Pinto model is a special plasticity model for the cyclic behavior of steel and is available for embedded reinforcements. It consists of a finite stress-strain relationship for branches between two subsequent reversal points and the parameters involved are updated after each load reversal. The modulus of elasticity was 406GPa, and the yield stress was 549MPa and 295MPa for longitudinal reinforcement and stirrups, respectively.

Table 1. Mechanical properties of Engineering masonry model

Elastic parameters	
Modulus of elasticity-X direction (GPa)	7
Modulus of elasticity-Y direction (GPa)	3.37
Shear modulus (GPa)	1.38
Mass density (Kg/m^3)	800
Cracking : head joint failure	
Tensile strength normal to the bed joint (MPa)	0.5
Residual tensile strength (MPa)	0.2
Fracture energy in tension (N/mm)	0.05
Crushing parameters	
Compressive strength (MPa)	5.1
Fracture energy (N/mm)	40
Factor at maximum compressive stress	4
Compressive unloading factor	0.2
Shear failure parameters	
Cohesion (MPa)	0.71
Shear fracture energy (N/mm)	1
Friction angle (degree)	20

Table 2. Mechanical properties of Total strain crack model for glass and carbon TRM

Total strain crack model with fiber reinforced concrete		
	Glass –TRM	Carbon-TRM
Elastic modulus (GPa)	30.00	34.00
Poison ratio	0.2	0.2
Mass density (Kg/m^3)	2400	2400
Total crack strain model	**Crack orientation Rotating**	
Tensile behavior	**Fib Fiber Reinforced Concrete**	
Tensile strength (MPa)	2.72	5.57
Tensile stress point I (MPa)	2.72	5.57
Strain at point I (%)	0.00009	0.00017
Tensile stress point J (MPa)	2.72	5.57
Tensile strain point J (%)	0.0021	0.001
Tensile stress point **k**(MPa)	12	15
Tensile strain point K (%)	0.015	0.007
Ultimate strain (%)	0.015	0.007
Crack band width	Rotating	
Compressive behavior	**Fib model code for concrete structure 2010**	
Compressive strength (MPa)	18	18
Strain at maximum stress (%)	0.021	0.021
Strain at ultimate stress(%)	0.035	0.035

The masonry infill wall material model used is the Engineering Masonry model, which is a smeared failure model and it has a total-strain based continuum model that covers tensile, shear and compression failure modes. The Engineering Masonry model describes the unloading behaviour assuming a linear unloading for compressive stresses with initial elastic stiffness. In addition, a shear failure mechanism based on the standard Coulomb friction failure criterion is included in the model. The Engineering Masonry model requires large number of mechanical properties and most of these properties were not measured in the experimental case study. These mechanical properties were taken from the literature. The model is defined in DIANA FEA with the parameters as shown in Table 1. The tensile strength normal to the bed joint was taken as 0.5 MPa according to Lourenço [32] and Rots [33] and the residual tensile strength was specified at 40% of the tensile strength. The tensile strength of the joint is still a subject of

research and therefore the tensile behavior parameters have been assumed according to the information provided by the respective experimental testing reports or related references.The compressive fracture energy and the tensile energy were calculated according to Rots [40]. The cohesion was obtained 1.5 times larger than the tensile strength according to the relation that was proposed by Cur [41]. The shear fracture energy was equal to ten times smaller of the cohesion as proposed by Lourenço [39]. The friction coefficient was chosen so that the ratio between the specimen compressive and tensile strengths was about ten, which ratio is often found for masonry units.

The TRM material model that was chosen is the Total Strain crack model with Fiber reinforced concrete model (*fib*) for tensile behavior [35,43]. The *fib* Model Code for Concrete Structures 2010 model was chosen for the compressive behavior of the TRM. Besides the definition of basic properties, like Young's modulus, the total crack strain model requires input parameters for the composite material behavior in tension and compression. The Fiber reinforced concrete model (*fib*) was specified as a function of the total strain. With the fiber reinforced concrete curve the cracking of concrete is initiated at the strain when the tensile strength is reached. In addition, the compressive and ultimate strain were obtained from CEB-FIP model code [35]. The model is defined in DIANA FEA with the parameters as shown in Table 2 and the tensile cyclic behavior of glass-TRM is shown in Fig. **5(b).**

The gap between the frame and masonry infill could significantly influence the overall behavior of the masonry infill RC frame. An interface gap model, plasticity based and proposed by Lourenço and Rots [38] was used for the interface elements describing the connection between the masonry infill wall and the bounding RC frame. The model includes a tension cut-off for tensile failure (mode I), a Coulomb friction envelope for shear failure (mode II) and a gap mode for compressive failure. The fracture of the interface is controlled by its tension mode, shear behaviour by Coulomb friction behaviour and crushing by the gap in compression mode. One drawback regarding the use of this interface model is the lack of material properties, as no data were available regarding the behaviour of the interface between the masonry infill and the frame. Therefore, it was decided to define the material properties of the interface by fitting the numerical results to the experimental results obtained for the experimental case study. The interfaces normal modulus was 6KN/mm³ and 3 KN/mm³ for perpendicular (y-direction) and longitudinal (x-direction) direction, respectively. The interface shear modulus was 0.06 KN/mm³ and 0.03 KN/mm³ for y-direction and x-direction, respectively. Furthermore, the interface friction was 30º for both directions.

3.2 Type of element and mesh

DIANA offers a broad range of element types for modelling brittle and quasi-brittle materials. The concrete frame, masonry infill wall and TRM were modelled with eight-node quadrilateral isoperimetric plane stress elements (CQ16M). The steel reinforcement in the frame was modeled with two-node bar elements and they were connected to the eight-node concrete elements at the two external nodes. Fig. (**6a**) shows both elements.

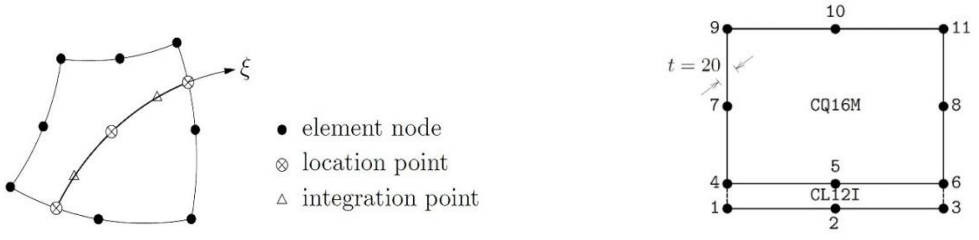

(a) (b)

Figure 6 : Elements used in the model: (a) CQ16M and steel reinforcement elements and (b) position of nodes of CQ16M and CL12I element.

The nonlinearity between masonry infill and RC frame zone was introduced with a 2D line interface element. The interface between the infill wall and the frame was modeled by the 3-point line interface element (CL12I) capable of modeling cohesion, separation, and cyclic behavior. The CL12I (Fig. **6b**) element is an interface element between two lines in a two-dimensional configuration. The squared mesh is preferred in FE models [42] and therefore in this case study the shape of the 2D elements were kept rectangular with nearly equal sides.

The way that the TRM elements are connected with the infill wall and with the concrete elements influence the TRM-masonry-infilled frame model behavior. The glass-TRM plane stress elements were connected with the nodes of infill-wall plane stress elements. The carbon-TRM plane stress elements were connected with the nodes of concrete plane-stress element. At the interface of the first and second floor in the horizontal direction, the glass-TRM plane stress element was connected to the nodes of concrete plane stress element in order to take into account the anchors (full bond). In addition, in order to take into account the debonding of the TRM from the beam at the first floor, the glass-TRM elements were connected to the nodes of the infill wall element instead of the nodes of the concrete element.

3.3 Type of loading and constrains

The model was loaded with a constant axial load on the top of the columns to simulate the dead load and with imposed cyclic horizontal displacement as shown in Fig**. 4(b**). The loading process during the numerical analysis simulated as closely as possible the experimental loading by using point prescribed deformation load. All nodes at the base of the masonry-infill RC frame were restrained by preventing any translation in the x and y-directions to simulate the strong foundation beam that was used in the experimental case study.

3.4 Type of analysis and convergence

Two types of analysis were performed: eigenvalue analysis and nonlinear structural cyclic analysis (deformation control). To perform nonlinear cyclic analysis a two phased analysis was selected. In the first phase the self-weight and the additional dead load of the structure were imposed. In the second phase, a quasi-static implicit, material non-linear analysis was performed with the a secant iteration scheme. The automatic incrementation procedure is used in which both the number of steps and the corresponding step size are automatically computed. The energy-based convergence criterion is applied with standard DIANA FEA tolerance values (0.0001). The continuation option was activated. The numerical model was calibrated to the experimental results by varying the parameters of the engineering masonry and interface mode.

4 FINITE ELEMENT MODEL RESULTS

In this part of the paper, the results of the eigen value analysis and nonlinear structural cyclic analysis are presented. The fundamental period of the bare frame and of the masonry-infilled RC frame with and without TRM is presented in Table 3 and they are in good agreement with the experimental ones.

Table 3. Comparison of experimental and numerical fundamental period

Fundamental period (Seconds)	**Bare frame**	**Masonry-infilled RC frame**	**TRM strengthened Masonry-infilled RC frame**
Experiment	0.24	0.06	0.047
Model	0.23	0.062	0.049

The global results obtained from TRM-strengthened masonry-infilled RC frame model, subjected to cyclic nonlinear analysis, are shown in Fig. (**7a**), which illustrates the experimental (black line) and numerical model (red line) response curves for the TRM masonry-infilled frame. In addition, the base shear in relation to the load step and the top story displacement vs. load step are presented in Fig. **7(b**) and Fig.**7(c**), respectively.

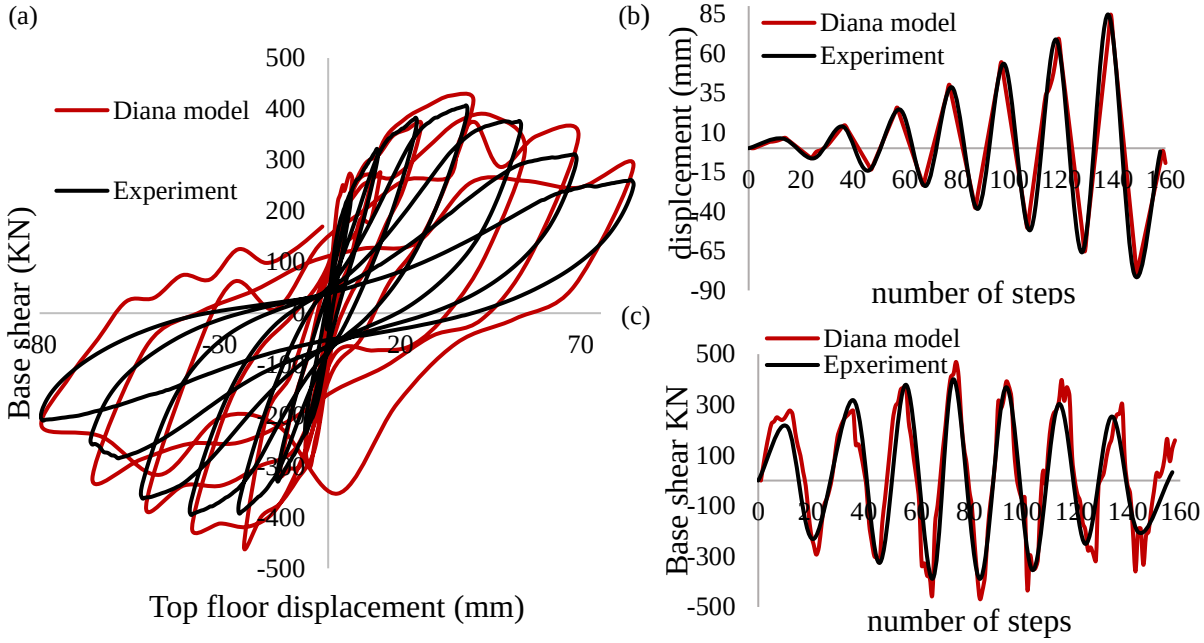

Figure 7 : Comparison between experiment and model results in terms of (a) base shear-top floor displacement hysteric curves, (b) base shear in relation to the load step and (c) and third story displacement in relation to the load step.

A comparison between numerical and experimental results for masonry-infilled RC frame is given in Fig. **8 (a)** and **(b)** in terms of global lateral stiffness and cumulative hysteretic energy, respectively. As illustrated in Fig. **8 (a)** and **(b)** the agreement between modeling and test results is satisfactory.

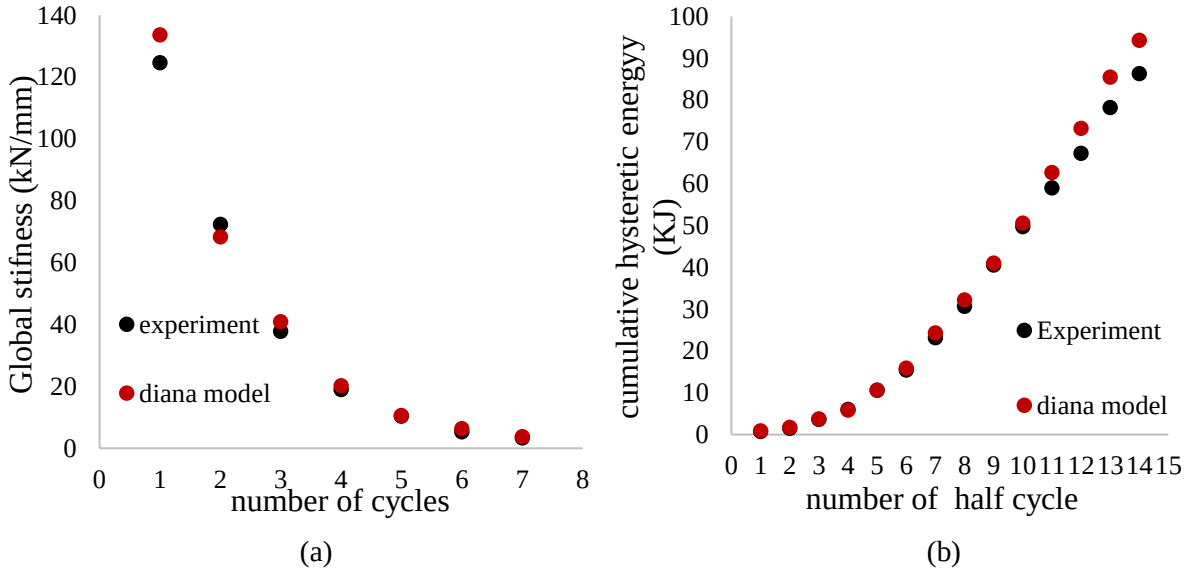

Figure 8: Comparison between analysis and experimental results for masonry- infilled frame in terms of the (a) global lateral stiffness per cycle and (b) cumulative global hysteretic energy.

Numerical results and experimental data of the TRM strengthened masonry-infilled RC frame have been compared and are in excellent agreement with the experimental ones regarding initial stiffness, ultimate stiffness, maximum shear force capacity and energy absorption in a cycle.

Based on the results from Fig.(**8c)** and Fig.(**9b**), the shear-force capacity and the energy absorption for the last cycle of loading is overestimated 15% and 12% respectively. This might depend on the analysis convergence and on the nonlinearities that were introduced in the last cycle of unloading.

Figure (**9a)** shows the cracking that occurred at the first floor during the fifth cycle of loading and unloading in the experimental case study and Fig. (**9b**) shows thee crack width in the numerical model during the fifth cycle of loading and unloading. The crack width in the numerical model shows that the cracks have the same location as observed in the experiment.

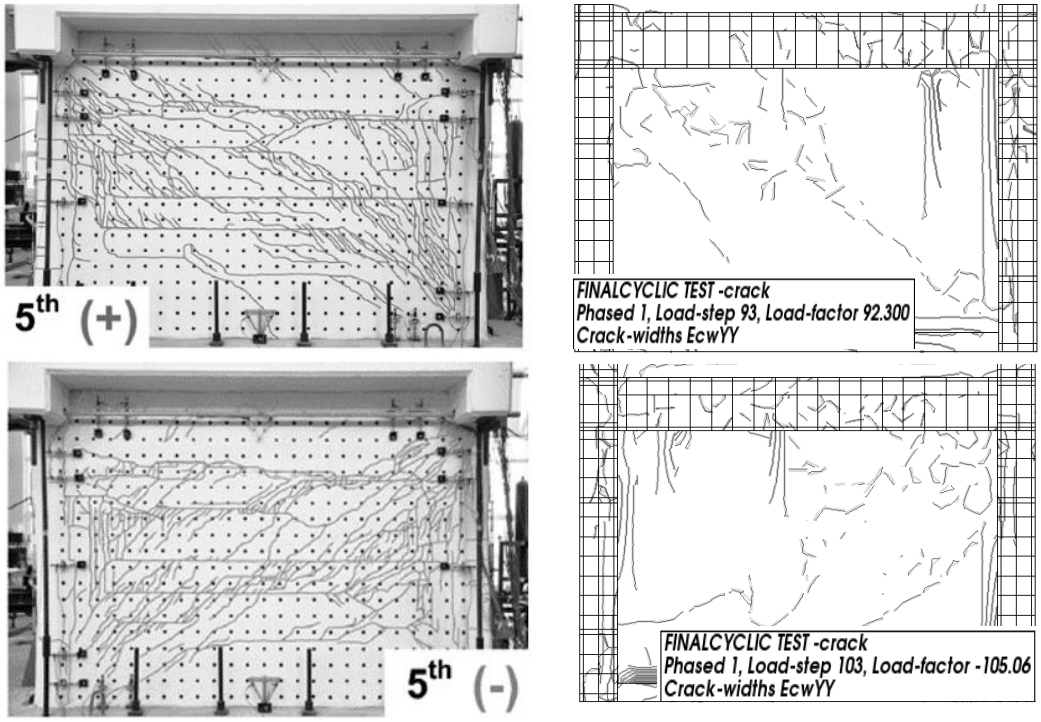

(a) (b)

Figure 9: (a) Crack patterns of TRM strengthened masonry-infilled frame test specimen and (b) crack widths in the numerical model during the fifth cycle of loading (positive and negative).

The results from the numerical model show the damage of the first story after the end of the test (Fig.**10**), which is the same damage that was observed in the experiment upon test completion.

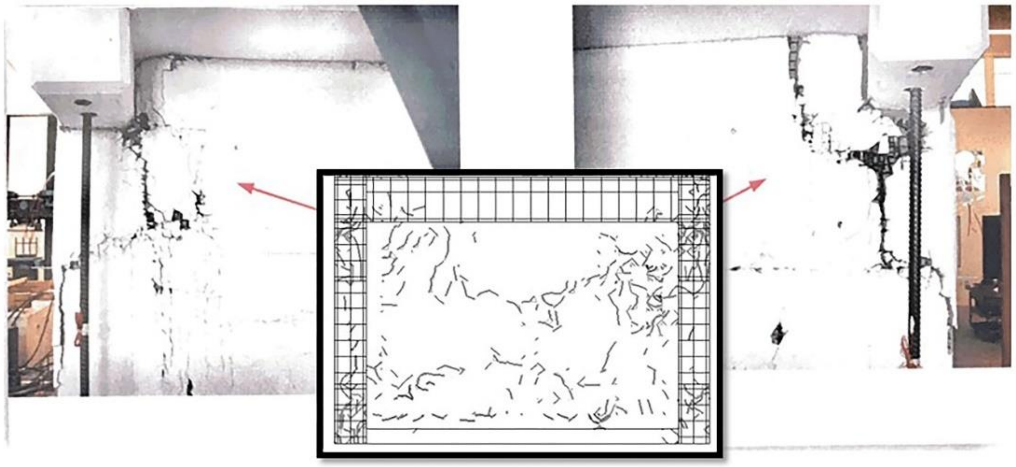

Figure 10 : Damage of first story after the end of the test and the rupture of TRM at the top end of first story's columns

5 CONCLUSION

This paper presents a numerical model that simulates the nonlinear cyclic-behavior of a TRM strengthened masonry-infilled RC frame subjected to in-plane actions in DIANA FEA software. The present study identifies suitable numerical constitutive models of each component of the structural system in order to create a numerical tool to model masonry infilled RC frames strengthened with TRM under in-plane cyclic loading. The calibration was based on the experimental test performed by Koutas [32]. Some of the material properties, especially for the masonry and for the interface were obtained from the literature [35,38].

Simulation results of the TRM strengthened masonry-infilled RC frame have been compared to the experimental ones with excellent agreement regarding the fundamental periods the initial stiffness, the ultimate stiffness and the maximum shear-force capacity. The crack-patterns show in general good agreement with the experiment, with respect to location and orientation of the cracks. TRM jacketing proved by experimental and numerical studies that is effective in large shear deformations through the development of a multi-crack pattern and by introducing an efficient load transferring mechanism at the local level.

It can be concluded that this model is a reliable model of the behavior of TRM strengthened masonry-infilled RC frame, with acceptable mismatch between the test and simulation results is observed. In particular the energy absorption and maximum shear-force capacity in the last cycle of loading is overestimated compared to experimental results, which may be attributed to high nonlinearities at that stage. In the future, this proposed numerical model which simulates the nonlinear behavior of TRM strengthened masonry-infilled RC frame will be used to perform numerical experiments through a parametric study to quantify the effect of critical parameters which are capable of affecting the performance of masonry-infilled structures reinforced with TRM. This will expand the results' database and will allow the development of design guidelines for a new strengthening technique on masonry-infilled RC frames using TRM.

6 REFERENCES

[1] I. K. and P. B. S. Andreas Stavridis, "Shake-table tests of a three-story reinforced concrete frame with masonry infill walls," *Earthq. Eng. Struct. Dyn.*, vol. 44, no. 11, pp. 657–675, 2012.

[2] M. N. Fardis and T. B. Panagiotakos, “Seismic design and response of bare and masonry-infilled reinforced concrete buildings. Part II: Infilled structures,” *J. Earthq. Eng.*, vol. 1, no. 3, pp. 475–503, 1997.

[3] J. Mehrabi, A., Benson Shing, P., Schuller, M., and Noland, “Experimental Evaluation of Masonry-Infilled RC Frames,” *Journal of Structural Engineering*, vol. 122, no. 3. pp. 228–337, 1996.

[4] F. Decanini, L.D., Gavarini, C. and Mollaioli, “Seismic Performance of Masonry Infilled R/C Frames,” *13th World Conference on Earthquake Engineering*. August 1-6, Canada, p. 165, 2004.

[5] V. Palieraki, C. Zeris, E. Vintzileou, and C. E. Adami, “In-plane and out-of plane response of currently constructed masonry infills,” *Eng. Struct.*, vol. 177, no. August, pp. 103–116, 2018.

[6] M. Donà, M. Minotto, E. Saler, G. Tecchio, and F. da Porto, “Combined in-plane and out-of-plane seismic effects on masonry infills in RC frames,” *Ing. Sismica*, vol. 34, no. Special Issue, pp. 157–173, 2017.

[7] G. Zuccaro, F. Dato, F. Cacace, D. D. de Gregorio, and S. Sessa, “Seismic collapse mechanisms analyses and masonry structures typologies: A possible correlation,” *Ing. Sismica*, vol. 34, no. 4, pp. 121–149, 2017.

[8] Federal Emergency Management Agency, “Evaluation of Earthquake Damaged Concrete and Masonry Wall Buildings-,” *FEMA 306,Applied Technology Council (ATC-43 Project)*. p. 250, 1998.

[9] P. G. Asteris, D. J. Kakaletsis, C. Z. Chrysostomou, and E. E. Smyrou, “Failure modes of in-filled frames,” *Electron. J. Struct. Eng.*, vol. 11, no. March 2016, pp. 11–20, 2011.

[10] P. B. Shing and A. B. Mehrabi, “Behaviour and analysis of masonry-infilled frames,” *Prog. Struct. Eng. Mater.*, vol. 4, pp. 320–331, 2002.

[11] C. Z. Chrysostomou and P. G. Asteris, “On the in-plane properties and capacities of infilled frames,” *Eng. Struct.*, vol. 41, pp. 385–402, 2012.

[12] C. Syrmakezis and P. Asteris, “Influence of infilled walls with openings to the seismic response of plane frames,” *Proc. 9th Can. Mason. Symp*, 2001.

[13] Y.-W. L. Chiou, Yaw-Jeng Jyh-Cherng Tzeng, “Experimental and analytical study of masonry infilled frames,” *J. Struct. Eng.*, vol. 125, no. 10, pp. 1109–1117, 1999.

[14] A. A. Costa and C. S. Oliveira, “O grande sismo de sichuan:impactos e licoes para futuro,” *8º congressi de sismologia e engenharia sismica*, no. C. pp. 1–31, 2010.

[15] X. Romão *et al.*, “Field observations and interpretation of the structural performance of constructions after the 11 May 2011 Lorca earthquake,” *Eng. Fail. Anal.*, vol. 34, no. 2, pp. 670–692, 2013.

[16] H. Kaplan and Y. Salih, “Seismic Strengthening of Reinforced Concrete Buildings,” *Earthquake-Resistant Struct. - Des. Assess. Rehabil.*, vol. 1, no. February, pp. 407–428, 2012.

[17] R. Kumar, Y. Singh, and R. Deoliya, “Review of Retrofitting Techniques for Masonry Infilled RC Frame Buildings,” *Trends and Challenges in Structural Engineering and*

Construction Technologies, vol. 1, no. February. pp. 284–296, 2009.

[18] C. J. J. Albert, M.L., Elwi, A.E., "Strengthening of Unreinforced Masonry Walls Using FRPs," *ASCE J. Compos. Constr.*, pp. 76–84, 2001.

[19] Y. A. Almusallam, T.H., Al-Salloum, "Behavior of FRP Strengthened Infilled Walls Under In-Plane Seismic Loading," *ASCE J. Compos. Constr.*, pp. 308–318, 2007.

[20] El-Dakhakhni, "Experimental and Analytical Seismic Evaluation of Concrete Masonry-Infilled Steel Frames Retrofitted using GFRP Laminates," 2002.

[21] M. A. Elgawady, P. Lestuzzi, and M. Badoux, "Rehabilitation of Unreinforced Brick Masonry Walls Using Composites," *Geotech. Geol. Eng.*, vol. 1, no. 3, pp. 413–422, 1986.

[22] M. ElGawady, M., Lestuzzi, P., and Badoux, "In-Plane Seismic Response of URM Walls Upgraded with FRP," *Compos. Struct.*, vol. 8, pp. 254–535, 2005.

[23] P. B. Foster, J. Gergely, D. T. Young, W. M. Mcginley, and A. Corzo, "Repair Methods for Unreinforced Masonry Buildings Subject to Cyclic Loading," *ACI Spec. Publ.*, pp. 289–306, 2005.

[24] K. Hamoush, S.A., McGinley, M.W., Mlakar, P., Scott, D., and Murray, "Out-ofPlane Strengthening of Masonry Walls with Reinforced Composites," *ASCE J. Compos. Constr.*, vol. 5, no. 3, pp. 139–145, 2001.

[25] M. K. . Tan, K.H. and Patoary, "Strengthening of Masonry Walls Against Outof-Plane Loads Using Fiber-Reinforced Polymer Reinforcement," *ASCE J. Compos. Constr.*, vol. 8, no. 1, pp. 79–87, 2004.

[26] TC Triantafillou, "Strengthening of masonry structures using epoxy-bonded FRP laminates," *ASCE J. Struct. Eng.*, pp. 104–11, 1998.

[27] V. C. L. Kim, Y.Y., Kong, H.J., "Design of Engineered Cementitious Composite Suitable for Wet-Mixture Shotcreting," *ACI Mater. J.*, vol. 100, no. 6, pp. 511–518, 2003.

[28] M. A. Kyriakides and S. Billington, "Seismic Retrofit of Unreinforced Masonry Infills in Non-Ductile Reinforced Concrete Frames Using Engineered Cementitious Composites," *Dept. Civ. Environ. Eng.*, vol. 3., no. March, 2011.

[29] M. A. Kyriakides and S. L. Billington, "Seismic Retrofit Of Masonry-Infilled Non-Ductile Reinforced Concrete Frames Using Sprayable Ductile Fiber-Reinforced Cementitious Composites," *14 World Conf. Earthq. Eng.*, no. April, 2008.

[30] C. G. Papanicolaou, T. C. Triantafillou, M. Papathanasiou, and K. Karlos, "Textile reinforced mortar (TRM) versus FRP as strengthening material of URM walls: out-of-plane cyclic loading," *Mater. Struct.*, vol. 41, no. 1, pp. 143–157, 2007.

[31] T. T. C. Papanicolau, "Textile-reinforced mortar versus FRP as strengthening material of URM walls: In-plane cyclic loading," *Mater. Struct.*, pp. 1081–1097, 2007.

[32] L. Koutas, S. N. Bousias, and T. C. Triantafillou, "Seismic Strengthening of Masonry-Infilled RC Frames with TRM: Experimental Study," *J. Compos. Constr.*, vol. 19, no. 2, p. 04014048, Aug. 2014.

[33] L. Koutas, T. Triantafillou, and S. Bousias, “Analytical Modeling of Masonry-Infilled RC Frames Retrofitted with Textile-Reinforced Mortar,” *J. Compos. Constr.*, vol. 19, no. 5, pp. 1–14, 2014.

[34] I.Sanya, “Comparison of Nonlinear Finite Element Modeling Tools for Structural Concrete.” pp. 1–56, 2006.

[35] Fib, “Model code 2010 Vol.1,” no. 1. pp. 247–278, 2010.

[36] J. A. N. G. Rots, “Smeared and discrete representations of localized fracture,” *Int. J. Fract.*, vol. 51, pp. 45–59, 1991.

[37] J. Lourenço, P. and Rots, “A plane stress softening plasticity model for orthotropic materials,” vol. 40, no. February 1996, pp. 4033–4057, 1997.

[38] J. Lourenço, P. and Rots, “Multisurface Interface Model for Analysis of Masonry Structures,” *J. Eng. Mech.*, vol. 9, no. September, pp. 660–688, 1997.

[39] P. B. Lourenço, “A user/programmer guide for the micro-modelling of masonry structures,” *TNO Build. Constr. Res. - Comput. Mech.*, no. 03, 1996.

[40] G.Rots, “DIANA Validation report for Masonry modelling,” netherlands, 2017.

[41] C.Cur, “Structural masonry: an experimental/numerical basis for practical design rules,” Gouda, The Netherlands., 1994.

[42] K. Ho-Le and An, “Finite element mesh generation methods : a review and classification,” *Comput. Des.*, vol. 20, no. I, pp. 27–38, 1988.

[43] Diana fea, “User ’ s Manual Material Library.” pp. 1–696, 2010.